JMSR 1(3) (2025)

Journal of Material Science and Radiation

https://journals.balaipublikasi.id/jmsr

Comparative Characterisation of Structural and Superconducting Properties of Y-123 and Y-247 Synthesised by Thermal Treatment at 980 °C

Siew Hong Yap[1], Tai Pao Er[1], Mohd Mustafa Awang Kechik[1*], Muhammad Khalis Abdul Karim[1], Hussien Baqiah[2], Soo Kien Chen[1], Kean Pah Lim[1], Muhammad Kashfi Shabdin[1], Nurhidayah Mohd Hapipi[1], Aliah Nursyahirah Kamarudin[1], Arebat Ryad Alhadei Mohamed[1], Aris Doyan[3], Abdul Halim Shaari[1]

[1]Superconductor & Thin Films Laboratory, Department of Physics, Faculty of Science, Universiti Putra Malaysia, 43400 UPM Serdang, Selangor, Malaysia
[2]Shandong Key Laboratory of Biophysics, Institute of Biophysics, Dezhou University, No. 566 University Rd. West, Dezhou, Shandong, China
[3]Department of Physics Education, Faculty of Teacher and Education, University of Mataram, Lombok, Indonesia

Received: July 12, 2025
Revised: November 19, 2025
Accepted: December 25, 2025
Published: December 31, 2025

Corresponding Author:
Mohd Mustafa Awang Kechik
mmak@upm.edu.my

DOI: 10.56566/jmsr.v1i3.425

Abstract: This study presents a comparative analysis of the structural and superconducting properties of $YBa_2Cu_3O_7-\delta$ (Y-123) and $Y_2Ba_4Cu_7O_{15}-\delta$ (Y-247) superconductors synthesised via a thermal treatment method at 980 °C. Metal nitrates were used as starting precursors, with polyvinylpyrrolidone (PVP) serving as a capping agent to enhance dispersion and control microstructure. X-ray diffraction (XRD) confirmed that Y-123 and Y-247 were the dominant phases in their respective samples, although minor peaks of $BaCuO_2$ were detected, indicating the presence of secondary phases. Scanning electron microscopy (SEM) revealed that Y-247 exhibited larger grain morphology and higher porosity than Y-123, suggesting that the chosen sintering temperature exceeds the thermal stability range for the Y-247 phase. Electrical resistivity measurements showed a single superconducting transition for both samples, with Y-123 exhibiting a sharper transition width (ΔT_c = 8.1 K) compared to Y-247, indicating better grain connectivity and phase uniformity. Energy dispersive X-ray spectroscopy (EDX) supported the elemental presence of Y, Ba, Cu, and O in both samples, though variations in stoichiometry were attributed to secondary phases. The observed expansion in the *c*-axis lattice of Y-247, combined with its higher porosity, points to oxygen loss during sintering, which contributes to the reduced superconducting performance. Overall, the results confirm that both Y-123 and Y-247 can be successfully synthesised using a simple and environmentally friendly thermal treatment method. However, Y-123 exhibits better structural integrity and superconducting performance at the high sintering temperature of 980 °C, making it a more promising candidate for large-scale production of bulk high-temperature superconductors.

Keywords: Microstructural; Phase formation; Superconducting transition width; Y-123; Y-247

Introduction

Yttrium Barium Copper Oxide (YBCO) superconductors are a widely studied family of high-temperature superconducting materials, valued for their potential in a range of practical applications, including power transmission, magnetic levitation systems, superconducting magnets, and energy storage technologies (Awang Kechik et al., 2009; Bahboh et al., 2019; Dihom et al., 2019; Khalid et al., 2020; Mohd Hapipi et al., 2017; Yap, Awang Kechik, Mohamed, et al., 2025). Their ability to conduct electrical current without

How to Cite:
Yap, S. H., Er, T. P., Kechik, M. M. A., Karim, M. K. A., Baqiah, H., Chen, S. K., … Shaari, A. H. Comparative Characterisation of Structural and Superconducting Properties of Y-123 and Y-247 Synthesised by Thermal Treatment at 980 °C. *Journal of Material Science and Radiation*, *1*(3), 83–90. https://doi.org/10.56566/jmsr.v1i3.425

resistance at liquid nitrogen temperatures (77K) makes them highly attractive for both industrial implementation and fundamental research (Bahboh et al., 2019; Kamarudin et al., 2021; Kamarudin et al., 2024; Mikheenko et al., 2010; Mohd Yusuf et al., 2019). Among the various rare-earth barium copper oxides, YBCO compounds have received particular attention due to their relatively high critical temperatures and their potential for large-scale synthesis and processing (Yap, Awang Kechik, et al., 2024).

Within this system, $YBa_2Cu_3O_{7-\delta}$ (Y-123) and $Y_2Ba_4Cu_7O_{15-\delta}$ (Y-247) represent two of the most investigated phases, each with distinct structural and superconducting characteristics. Y-123 typically adopts an orthorhombic crystal structure that contains single copper-oxygen chains, and it is known for its high critical temperature, often exceeding 90 K. However, it is also known to be sensitive to thermal fluctuations, which can lead to oxygen loss and reduced phase stability. In contrast, Y-247 comprises alternating structural units of Y-123, incorporating both single and double Cu–O chains (Kandyel et al., 2013). This more complex arrangement contributes to improved thermal and oxygen stability (Anand et al., 2004), and may enhance flux pinning behavior. Despite these advantages, the synthesis of high-purity Y-247 remains more challenging, often requiring high oxygen pressures or multiple processing steps (Nawazish et al., 2002). As a result, its study has been more limited compared to Y-123, especially in terms of scalable production routes.

The synthesis method used to prepare bulk Y-123 and Y-247 superconductors plays a critical role in determining their structural integrity and overall performance (Arebat et al., 2025; Mohamed Arebat et al., 2025). Common fabrication techniques include solid-state reaction (Barood et al., 2024), co-precipitation (Hapipi et al., 2018; Hapipi et al., 2019), and thermal treatment (Dzul-Kifli et al., 2022; Tan et al., 2023; Yap et al., 2023), which can significantly influence phase composition and microstructural development. Among these, thermal treatment has emerged as a promising approach for producing fine, homogeneous superconducting powders, particularly when sintering conditions are carefully optimized (Sah et al., 2024; Yap, Kechik, Shariff, et al., 2024). The sintering temperature, in particular, is a key parameter, as YBCO phases are known to be highly sensitive to thermal variations, which can directly impact both crystal structure and superconducting behavior (Yap, Kechik, Khoerunnisa, et al., 2024).

In this study, we present a comparative characterisation of Y-123 and Y-247 superconductors synthesised under identical conditions using a thermal treatment method at 980 °C. Metal nitrates were selected as precursor materials, while polyvinylpyrrolidone (PVP) was incorporated as a capping agent to improve dispersion and control the reaction environment. This synthesis approach offers a simpler, more environmentally sustainable alternative to conventional methods involving high-pressure oxygenation or toxic solvents. The primary aim of this work is to evaluate the influence of a high sintering temperature of 980 °C on the structural, microstructural, and superconducting properties of Y-123 and Y-247 compounds. Structural characterisation was conducted using X-ray diffraction, while scanning electron microscopy and four-point probe measurements were used to assess grain morphology and critical temperature, respectively. The findings offer new insight into the influence of synthesis conditions on each phase and assess the viability of thermal treatment as a green, scalable method for producing high-quality YBCO superconductors.

Method

Sample Preparation:

All metal nitrate chemicals used were of high purity (99.9%). The starting materials included yttrium(III) nitrate hexahydrate (99.9%), barium nitrate (99.9%), and copper(II) nitrate hemi-(pentahydrate) (98.0–102.0%). Polyvinyl pyrrolidone (PVP) was added as a capping agent, and deionised water was used as the solvent. The solution was stirred using a magnetic stirrer at 850 rpm for 2 hours at 80 °C. A light green solution was obtained, which was then dried at 110 °C for 24 hours. After drying, the resulting dark green lumps were ground and pre-calcined at 600 °C for 4 hours. The grey powder formed was then reground and calcined at 910 °C for 24 hours. The calcined powder was ground once more and pressed into pellets using a hydraulic press under uniform pressure. Finally, the pellets were sintered at 980 °C for 24 hours.

Sample Characterization:

All samples were characterised using an X-ray diffractometer (XRD) to identify the crystalline phases present in the Y-123 and Y-247 systems. Phase identification and crystallographic orientation were analysed using X'Pert Graphics software, with CuKα radiation (λ = 1.5406 Å) in the 2θ range of 20° to 80°. The superconducting transition temperature (T_c) was measured using a custom-built four-point probe (4PP) setup. The microstructural properties of the samples were examined using a LEO 1455 VP scanning electron microscope (SEM) equipped with an energy-dispersive X-ray (EDX) spectrometer. Prior to imaging, the samples were coated with a thin gold layer to minimise electrostatic charging. SEM analysis was carried out at an accelerating voltage of 20 kV under various magnifications. EDX was used to determine the elemental composition of selected regions. Grain size

and porosity were quantitatively analysed from the SEM micrographs using Image*J* software.

Results and Discussion

Phase Formation and Crystal Structure

Based on the XRD results presented in Figure 1, the major diffraction peaks observed correspond to the Y-123 and Y-247 phases for their respective samples. Both samples exhibit an orthorhombic crystal system, confirming the successful formation of the intended superconducting phases. As shown in Figure 1, the peak intensities and phase formations varying for both Y-123 and Y-247 samples. The highest intensity peak for Y-247 is located at the (013) plane, whereas for Y-123, the most intense peak is observed at the (103) plane. Comparatively, the main peak of Y-123, located at 2θ = 32.91°, exhibits a higher intensity than the main peak of Y-247 at 2θ = 32.76°. While Y-123 and Y-247 are the dominant phases in their respective samples, minor peaks corresponding to barium copper oxide ($BaCuO_2$) were also detected, indicating the presence of a secondary phase at low intensity.

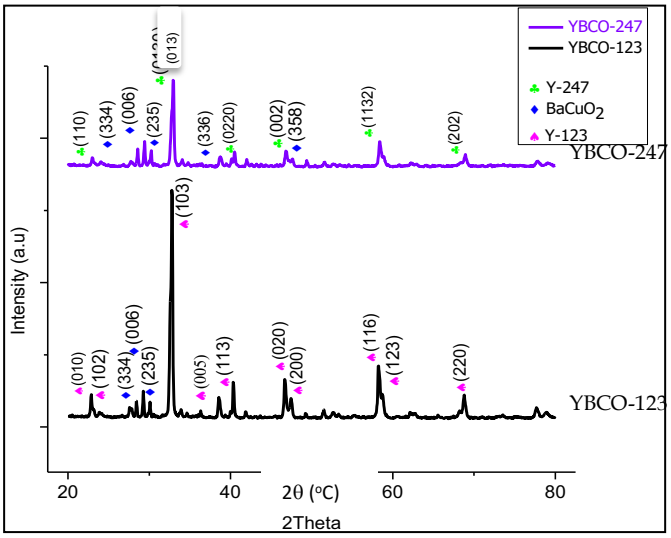

Figure 1. XRD pattern of pure Y-123 and pure Y-247 which sintered at temperature 980 °C for 24 hours.

Table 1 presents the lattice parameters and unit cell volumes obtained for the Y-123 and Y-247 samples. A significant difference in the lattice constants is observed between the two phases, particularly along the *c*-axis, where Y-247 exhibits a substantially larger value compared to Y-123. As a result, the unit cell volume and orthorhombicity of Y-247 are markedly higher, with the *c*-axis lattice parameter being approximately four times greater than that of Y-123. The higher orthorhombicity value observed in Y-123 indicates a greater oxygen content, which corresponds to an increased hole concentration when compared to Y-247.

Table 1. The lattice constants for sample Y-123 and Y-247.

Sample	Lattice Constant			Orthorhombicity	Volume of unit cell (10^6 pm^3)
	a (Å)	*b* (Å)	*c* (Å)		
YBCO-123	3.832	3.883	11.670	0.006611	173.646
YBCO-247	3.808	3.834	50.679	0.003402	739.901

Table 2 summaries the volume fraction, crystallite size, and lattice strain of the phases present in the Y-123 and Y-247 samples. The Y-123 sample exhibited a higher volume fraction of the Y-123 phase (85.4%), indicating a more concentrated and dominant phase compared to the Y-247 phase in the Y-247 sample. In contrast, Y-247 showed a higher volume fraction of the secondary phase, BaCuO2, than Y-123. The crystallite size of the Y-123 phase was found to be larger than that of Y-247, while the lattice strain displayed an inverse trend. The higher lattice strain observed in Y-247 may be attributed to increased lattice distortion, possibly caused by the higher concentration of $BaCuO_2$ in the sample.

Table 2. Volume fraction, crystallite size and lattice strain of the phases present on sample for Y-123 and Y-247.

Sample	Volume fraction (%)			Crystallite size (Å)	Lattice strain (%)
	Y-123	Y-247	BaCuO2		
YBCO-123	85.4	-	14.6	663	0.192
YBCO-247	-	81.4	18.6	528	0.239

Figures 2, 3, and 4 present scanning electron microscopy (SEM) images of the surfaces of Y-123 and Y-247 superconducting bulk samples at magnifications of 1500×, 3000×, and 5000×, respectively. Both samples exhibit thin, plate-like grains arranged in compact layers; however, the grain size in the Y-123 sample appears noticeably smaller than that of Y-247. In Figure 2, dark voids observed in the micrograph indicate the presence of porosity. A comparison of Figures 2 and 3 clearly reveals that the Y-247 sample contains a greater degree of porosity than Y-123. This difference in microstructure may be attributed to the use of a sintering temperature that exceeds the optimal range for Y-247, which is typically around 810 °C, as reported by Guo and colleagues in 1995 (Guo et al., 1995). Although the findings in this study differ from some previous reports, the observed reduction in grain size in both YBCO samples could be associated with the presence of secondary phases such as $BaCuO_2$, which may disrupt normal grain growth during sintering.

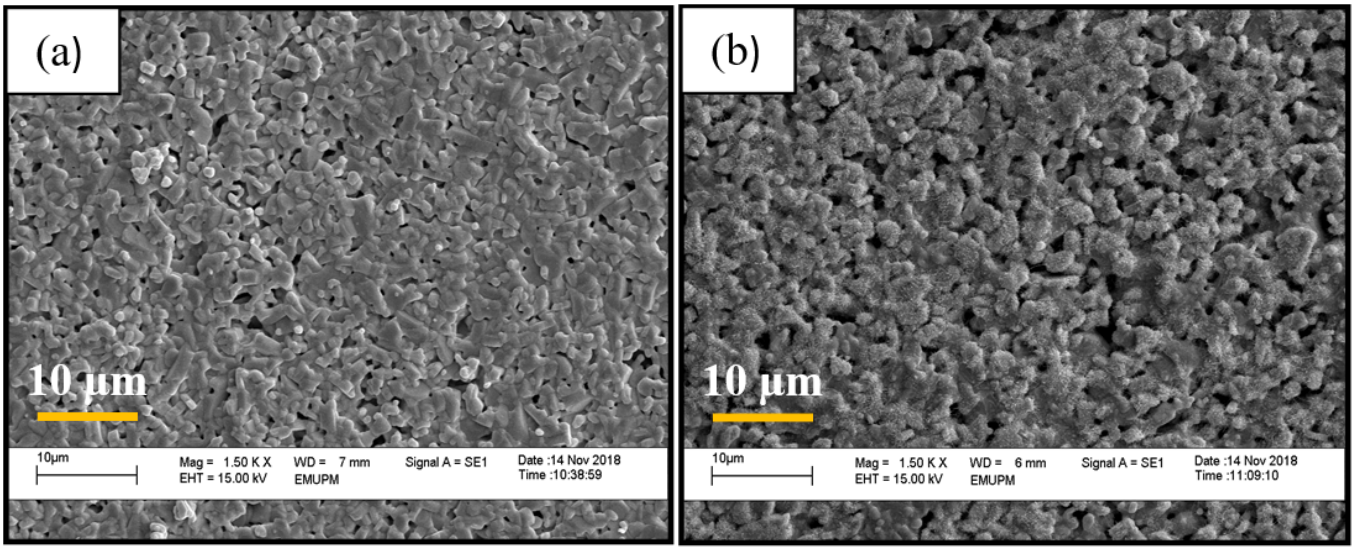

Figure 2. SEM micrographs for sample (a) Y-123 and (b) Y-247 at 1500x magnification on surface morphology.

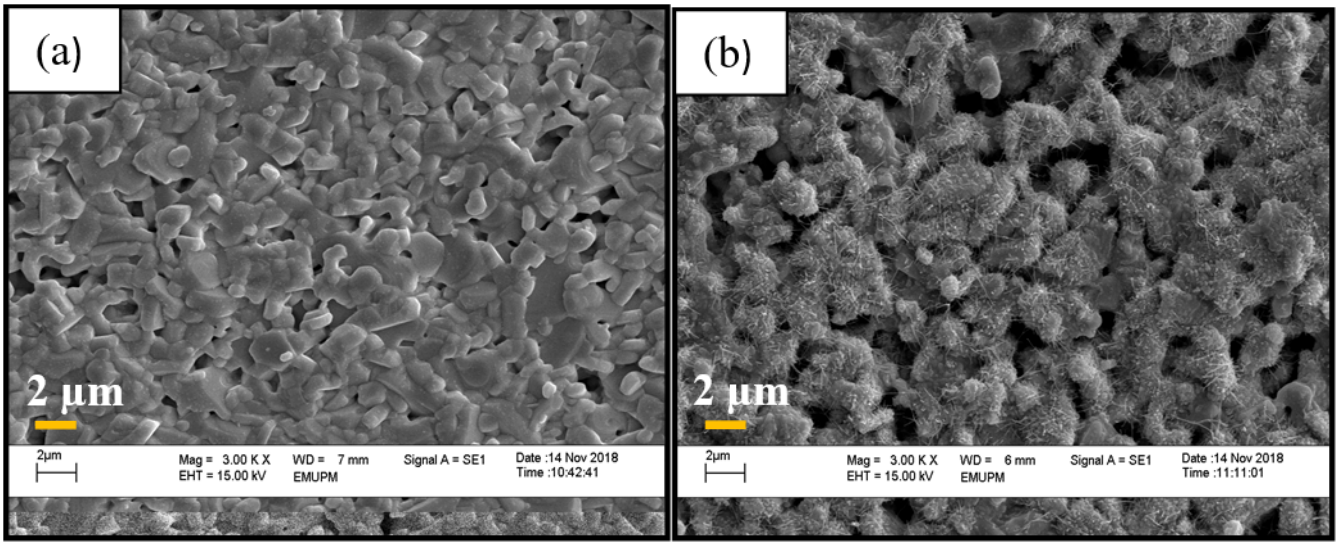

Figure 3. SEM micrographs for sample (a) Y-123 and (b) Y-247 at 3000x magnification on surface morphology.

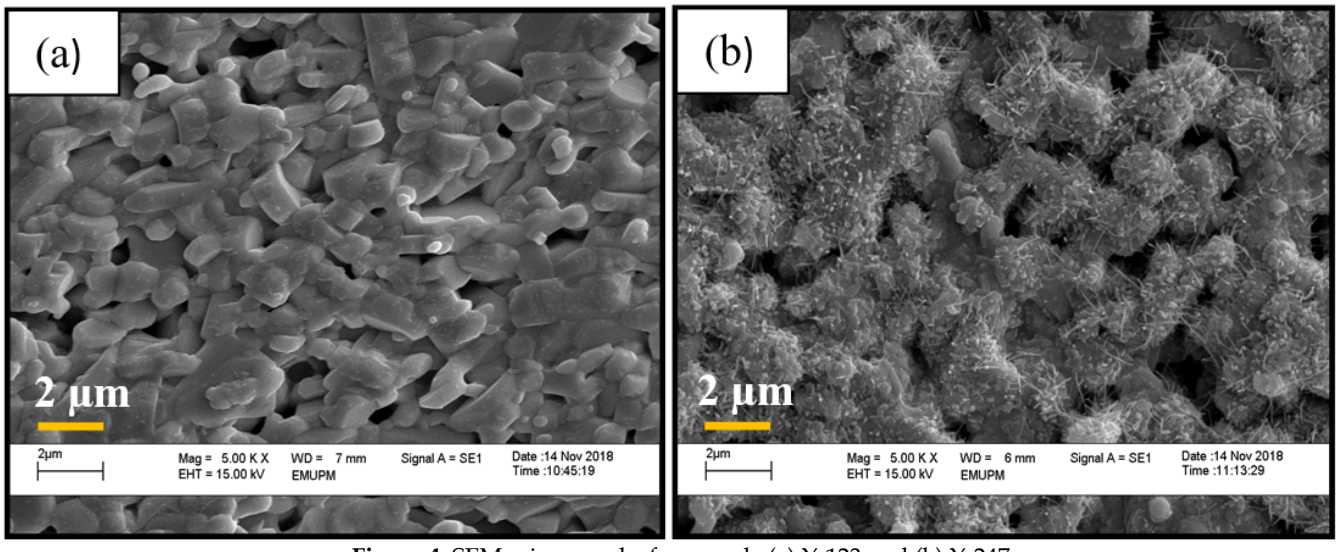

Figure 4. SEM micrographs for sample (a) Y-123 and (b) Y-247 at 5000x magnification on surface morphology

Table 3 presents the SEM results illustrating the effect of the sintering process on grain size in two different superconducting samples. Grain size measurements were obtained by averaging multiple values across representative regions of the microstructure. The average grain size for the Y-123 sample was found to be approximately 0.201 micrometres, which is smaller than that of Y-247, recorded at around 0.298 micrometres. In comparison to earlier studies that employed the thermal treatment method, larger grain sizes were reported—0.65 micrometres for Y-123 and 0.76 micrometres for Y-247 (Dihom et al., 2017). The reduction in grain size observed in this study may be attributed to the presence of secondary phases such as $BaCuO_2$, which can disrupt uniform grain growth.

As observed in Figures 2, 3, and 4, the Y-247 sample exhibits a greater degree of porosity compared to Y-123. This increased porosity likely contributes to the suppression of the T_c in the Y-247 sample, which measured lower than the expected value of 96 K. The open porous structure may facilitate oxygen loss during sintering, leading to oxygen deficiency in the lattice. This effect is further supported by data in Table 1, which shows that the c-axis lattice parameter exhibits more noticeable variation compared to the a and b axes. It is well established that oxygen loss causes expansion along the c-axis and an increase in unit cell volume, both of which are associated with a decrease in T_c (Khalida et al., 2013).

Table 3. The average size of the grains for both samples Y-123 and Y-247.

Sample	Average Size (μm)
YBCO-123	0.201
YBCO-247	0.298

Table 4 presents the EDX spectra results for Y-123 and Y-247 phases sintered at a high temperature of 980 °C. Peaks corresponding to the elemental composition of yttrium (Y), barium (Ba), copper (Cu), and oxygen (O) were successfully detected in both samples as shown in Figure 5. However, accurate interpretation of the elemental ratios in Y-123 and Y-247 was affected by the presence of secondary phases, such as $BaCuO_2$, which were confirmed through XRD analysis.

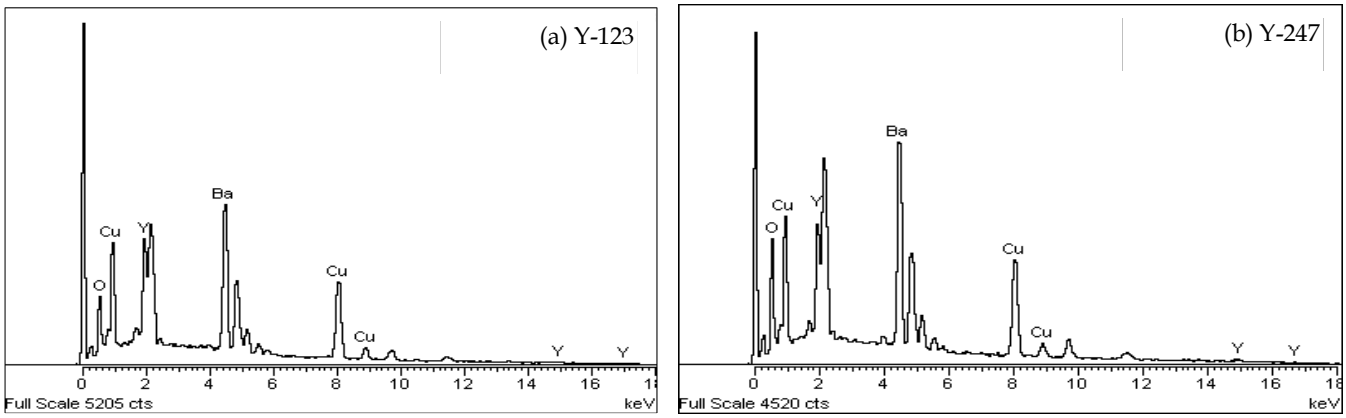

Figure 5. The EDX spectra line for (a) Y-123 and (b) Y-247 sintered at 980 °C.

Table 4. The ratio of $YBa_2Cu_3O_{7-x}$ and $Y_2Ba_4Cu_7O_{15-x}$ atomic percentage at same sintering condition and temperature.

Sample	Y (%)	Ba (%)	Cu (%)	O (%)	Ratio
Y-123	19.93	42.47	26.98	10.62	1: 2.13: 1.35: 0.53
Y-247	17.61	42.99	25.86	13.53	1: 2.44: 1.47: 0.76

Electrical transport properties

Figure 6 presents the normalised resistivity measurements for the Y-123 and Y-247 samples. Both samples exhibit a single sharp transition from the onset ($T_{c\text{-onset}}$) to the offset ($T_{c\text{-offset}}$) of superconductivity. This indicates that the grain connectivity in both samples remains reasonably intact, despite the presence of secondary phases such as $BaCuO_2$ in relatively high volume fractions, as reported in Table 2.

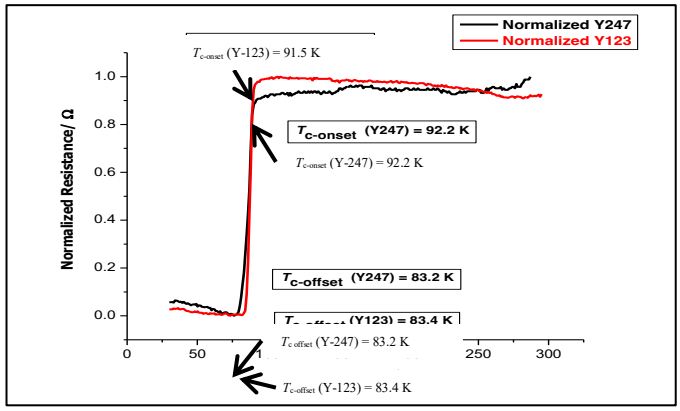

Figure 6. The four point probe results that show transition temperature of the Y-123 and Y-247 that sintered at 980 °C

The T_c of the Y-123 and Y-247 samples were determined from resistivity measurements, as summarised in Table 5.

Table 5. The variations of transition temperature (T_c) and the transition temperature range of both samples that sintered at same temperature and condition.

Sample	$T_{c\text{-onset}}$ (K)	$T_{c\text{-offset}}$ (K)	Temperature range (ΔT_c)
Y-123	91.5	83.4	8.1
Y-247	92.2	83.2	9.0

For the Y-123 sample, the onset and offset of the superconducting transition occurred at 91.5 K and 83.4 K, respectively. In comparison, the Y-247 sample exhibited a higher $T_{c\text{-onset}}$, but a broader transition width (ΔT_c), indicating a less sharp transition. A narrower superconducting transition range reflects stronger grain connectivity and superior superconducting behavior (Yap, Awang Kechik, Alhadei Mohamed, et al., 2025; Yap, Awang Kechik, et al., 2024). Based on this criterion, Y-123 demonstrates better superconducting performance than Y-247. These findings are consistent with previous work by X. Guo et al., who reported a T_c of approximately 96 K for Y-247 and around 92 K for Y-123 (Guo et al., 1995). However, the present study suggests that the sintering temperature of 980 °C is more favourable for Y-123, whereas Y-247 appears to degrade under these conditions. The apparent reduction in T_c for Y-247 in this work may be attributed to its porous microstructure, which can lead to the loss of vital oxygen during high-temperature sintering. As shown in Table 1, the *c*-axis lattice parameter exhibited a more pronounced change than the *a* and *b* axes, which aligns with findings by Khalida et al. (2013) , who reported that oxygen deficiency results in lattice expansion along the *c*-axis and a corresponding decline in T_c (Khalida et al., 2013).

Conclusion

In this study, bulk Y-123 and Y-247 superconductors were successfully synthesised via a thermal treatment method using metal nitrates as precursors and polyvinylpyrrolidone (PVP) as a capping agent. The results demonstrate that sintering at a high temperature of 980 °C significantly influences the structural, microstructural, and superconducting properties of both materials. XRD analysis confirmed the dominant phase formation of Y-123 and Y-247 in their respective samples, along with the presence of secondary phases such as $BaCuO_2$. SEM characterisation revealed that Y-247 exhibits a higher degree of porosity and larger grain size compared to Y-123, likely due to structural instability at elevated temperatures. Electrical resistivity measurements further showed that Y-123 displayed a narrower superconducting transition width (ΔT_c = 8.1 K), indicating better grain connectivity and phase homogeneity under high-temperature sintering. Overall, the findings suggest that Y-123 is more thermally stable and better suited for synthesis at 980 °C than Y-247, making it a more favourable candidate for high-temperature processing in practical applications.

Acknowledgments
Authors gratefully acknowledge financial support from the Ministry of Higher Education Malaysia (MOHE) for Fundamental Research Grant Scheme FRGS/1/2019/STG02/UPM/02/3 (5540282) Universiti Putra Malaysia.

Author Contributions
Conceptualization, Mohd Mustafa Awang Kechik and Siew Hong Yap; methodology, Siew Hong Yap and Tai Pao Er; software, Mohd Mustafa Awang Kechik, Soo Kien Chen, Muhammad Kashfi Shabdin and Kean Pah Lim; validation, Muhammad Khalis Abdul Karim , Arebat Ryad Alhadei Mohamed, Hussien Baqiah, Nurhidayah Mohd Hapipi; formal analysis, Tai Pao Er; investigation, Siew Hong Yap and Tai Pao Er; resources, Mohd Mustafa Awang Kechik, Soo Kien Chen and Kean Pah Lim; data curation, Siew Hong Yap, Aliah Nursyahirah Kamarudin and Tai Pao Er; writing—original draft preparation, Siew Hong Yap.; writing—review and editing, Siew Hong Yap, Mohd Mustafa Awang Kechik; visualization, Soo Kien Chen, Arebat Ryad Alhadei Mohamed and Abdul Halim Shaari; supervision, Mohd Mustafa Awang Kechik; project administration, Mohd Mustafa Awang Kechik; funding acquisition, Mohd Mustafa Awang Kechik. All authors have read and agreed to the published version of the manuscript.

Funding
This research was funded by Ministry of Higher Education Malaysia (MOHE) for Fundamental Research Grant Scheme FRGS/1/2024/STG05/UPM/02/4 Universiti Putra Malaysia, grant number 5540701

Conflicts of Interest
The funders had no role in the design of the study; in the collection, analyses, or interpretation of data; in the writing of the manuscript; or in the decision to publish the results.

References

Anand, S., & Srivastava, O. N. (2004). Formation and characterization of Y : 247 film through spray pyrolysis technique. *Bulletin of Materials Science*, *27*(2), 113-119. https://doi.org/10.1007/BF02708492

Arebat, R. A. M., Kechik, M. M. A., Kien, C. S., Pah, L. K., Baqiah, H., Hong, Y. S., Shaari, A. H., Zailani, T. H., Shariff, K. K. M., Shabdin, M. K., Karim, M. K. A., & Miryala, M. (2025). Influence of oxygen flow vs. ambient annealing on microstructure and superconducting properties of $YBa_2Cu_3O_{7-\delta}$ bulk ceramics. *Journal of Materials Science: Materials in Electronics*, *36*(12), 760. https://doi.org/10.1007/s10854-025-14827-7

Awang Kechik, M. M., Mikheenko, P., Sarkar, A., Dang, V. S., Hari Babu, N., Cardwell, D. A., Abell, J. S., & Crisan, A. (2009). Artificial pinning centres in $YBa_2Cu_3O_{7-\delta}$ thin films by $Gd_2Ba_4CuWO_y$

nanophase inclusions. *Superconductor Science and Technology*, *22*(3), 034020. https://doi.org/https://iopscience.iop.org/article/10.1088/0953-2048/22/3/034020/meta

Bahboh, A., Shaari, A. H., Baqiah, H., Kien, C. S., Kechik, M. M. A., Wahid, M. H., Abd-Shukor, R., & Talib, Z. A. (2019). Effects of $HoMnO_3$ nanoparticles addition on microstructural, superconducting and dielectric properties of $YBa_2Cu_3O_{7-\delta}$. *Ceramics International*, *45*(11), 13732-13739. https://doi.org/https://doi.org/10.1016/j.ceramint.2019.04.069

Barood, F., Awang Kechik, M. M., Miryala, M., Soo Kien, C., Kean Pah, L., Halim Shaari, A., & Baqiah, H. (2024). Effect of annealing temperature condition on the phase formation and electric proeprties of $YBa_2Cu_3O_{7-\delta}$ superconductor synthesised by thermal treatment method. *Solid State Science and Technology*, *31*(2), 63-70. Retrieved from https://myjms.mohe.gov.my/index.php/masshp/article/view/25639

Dihom, M. M., Shaari, A. H., Baqiah, H., Al-Hada, N. M., Chen, S. K., Azis, R. a. S., Awang Kechik, M. M., & Abd-Shukor, R. (2017). Effects of Calcination Temperature on Microstructure and Superconducting Properties of Y123 Ceramic Prepared Using Thermal Treatment Method. *Solid State Phenomena*, *268*, 325-329. https://doi.org/10.4028/www.scientific.net/SSP.268.325

Dihom, M. M., Shaari, A. H., Baqiah, H., Kien, C. S., Azis, R. S., Abd-Shukor, R., Al-Hada, N. M., Kechik, M. M. A., & Talib, Z. A. (2019). Calcium-Substituted $Y_3Ba_5Cu_8O_{18}$ Ceramics Synthesized via Thermal Treatment Method: Structural and Superconducting Properties. *Journal of Superconductivity and Novel Magnetism*, *32*(7), 1875-1883. https://doi.org/https://doi.org/10.1007/s10948-018-4905-3

Dzul-Kifli, N. A. C., Kechik, M. M. A., Baqiah, H., Shaari, A. H., Lim, K. P., Chen, S. K., Sukor, S. I. A., Shabdin, M. K., Karim, M. K. A., Shariff, K. K. M., & Miryala, M. (2022). Superconducting Properties of $YBa_2Cu_3O_{7-\square}$ with a Multiferroic Addition Synthesized by a Capping Agent-Aided Thermal Treatment Method. *Nanomaterials*, *12*(22), 3958. https://doi.org/10.3390/nano12223958

Guo, Y. X., Høier, R., Graf, T., & Genoud, J. Y. (1995). Processing related microstructure and superconductivity in YBCO-247. *Philosophical Magazine B*, *72*(4), 383-390. https://doi.org/10.1080/13642819508239093

Hapipi, N. M., Chen, S. K., Shaari, A. H., Kechik, M. M. A., Tan, K. B., & Lim, K. P. (2018). Superconductivity of Y_2O_3 and $BaZrO_3$ nanoparticles co-added $YBa_2Cu_3O_{7-\delta}$ bulks prepared using co-precipitation method. *Journal of Materials Science: Materials in Electronics*, *29*(21), 18684-18692. https://doi.org/https://doi.org/10.1007/s10854-018-9991-2

Hapipi, N. M., Chen, S. K., Shaari, A. H., Kechik, M. M. A., Tan, K. B., Lim, K. P., & Lee, O. J. (2019). AC susceptibility of $BaZrO_3$ nanoparticles added $YBa_2Cu_3O_{7-\delta}$ superconductor prepared via coprecipitation method. *Journal of Superconductivity and Novel Magnetism*, *32*(5), 1191-1198. https://doi.org/https://doi.org/10.1007/s10948-018-4829-y

Kamarudin, A. N., Awang Kechik, M. M., Miryala, M., Pinmangkorn, S., Murakami, M., Chen, S. K., Baqiah, H., Ramli, A., Lim, K. P., & Shaari, A. H. (2021). Microstructural, Phase Formation, and Superconducting Properties of Bulk $YBa_2Cu_3O_y$ Superconductors Grown by Infiltration Growth Process Utilizing the $YBa_2Cu_3O_y$ + $ErBa_2Cu_3O_y$ + $Ba_3Cu_5O_8$ as a Liquid Source. *Coatings*, *11*(4), 377. https://doi.org/10.3390/coatings11040377

Kamarudin, A. N., Miryala, M., Awang Kechik, M. M., Chen, S. K., Lim, K. P., Abdul Karim, M. K., Shabdin, M. K., & Shaari, A. H. (2024). Optimization of a heating pattern for single grain $(Y,Er)Ba_2Cu_3O_{7-x}$ by infiltration growth process. *Journal of Alloys and Compounds*, *984*, 173912. https://doi.org/https://doi.org/10.1016/j.jallcom.2024.173912

Kandyel, E., Salem, A., & Alqarni, A. (2013). Synthesis and Characterization of Doped $YBa_2Cu_4O_8$ Superconductor by Cd^{+2}. *Journal of Superconductivity and Novel Magnetism*, *26*(12), 3363-3368. https://doi.org/10.1007/s10948-013-2199-z

Khalid, N. A., Kechik, M. M. A., Baharuddin, N. A., Kien, C. S., Baqiah, H., Pah, L. K., Shaari, A. H., Talib, Z. A., Hashim, A., & Murakami, M. (2020). Carbon nanofibers addition on transport and superconducting properties of bulk $YBa_2Cu_3O_{7-\delta}$ material prepared via co-precipitation. *Journal of Materials Science: Materials in Electronics*, *31*(19), 16983-16990. https://doi.org/https://doi.org/10.1007/s10854-020-04255-0

Khalida, S., Fariesha, F., Azhan, H., & Yusainee, S. Y. (2013). Influence of Heat Treatments on Electrical Properties and Microstructure of 10% Mass Fraction of Sucrose YBCO Superconductor. *Malaysian Journal of Analytical Sciences*, *17*(1), 1-10. Retrieved from http://www.ukm.my/mjas/v17_n1/Khalida.pdf

Mikheenko, P., Abell, J. S., Sarkar, A., Dang, V. S., Kechik, M. M. A., Tanner, J. L., Paturi, P., Huhtinen, H., Babu, N. H., Cardwell, D. A., & Crisan, A.

(2010). Self-assembled artificial pinning centres in thick YBCO superconducting films. *Journal of Physics: Conference Series*, *234*(2), 022022. https://doi.org/10.1088/1742-6596/234/2/022022

Mohamed Arebat, R. A., Awang Kechik, M. M., Hong, Y. S., Kien, C. S., Pah, L. K., Baqiah, H., Barood, F., Humaidi, S., Peh, H. K., Shaari, A. H., Shabdin, M. K., & Miryala, M. (2025). Sm2O3-induced superconductivity enhancements in bulk Y-123 ceramics synthesized via a novel modified thermal decomposition method. *Journal of Materials Research and Technology*, *36*, 9168-9181. https://doi.org/https://doi.org/10.1016/j.jmrt.2025.05.065

Mohd Hapipi, N., Shaari, A. H., Kechik, M. M. A., Tan, K. B., Abd-Shukor, R., Mohd Suib, N. R., & Chen, S. K. (2017). Effect of Heat Treatment Condition on the Phase Formation of $YBa_2Cu_3O_{7-\delta}$ Superconductor. *Solid State Phenomena*, *268*, 305-310. https://doi.org/10.4028/www.scientific.net/SSP.268.305

Mohd Yusuf, N. N., Awang Kechik, M. M., Baqiah, H., Soo Kien, C., Kean Pah, L., Shaari, A. H., Wan Jusoh, W. N. W., Sukor, A., Izzati, S., & Mousa Dihom, M. (2019). Structural and superconducting properties of thermal treatment-synthesised bulk $YBa_2Cu_3O_{7-\delta}$ superconductor: Effect of addition of SnO_2 nanoparticles. *Materials*, *12*(1), 92. https://doi.org/https://doi.org/10.3390/ma12010092

Nawazish, A. K., Mazhar, M., & Asghari, M. (2002). A novel method for the direct synthesis of the Y2Ba4Cu7O15−x superconductor. *Superconductor Science and Technology*, *15*(4), 577. https://doi.org/10.1088/0953-2048/15/4/316

Sah, N. A. M. I. A., Kechik, M. M. A., Kien, C. S., Pah, L. K., Shaari, A. H., Shabdin, M. K., Karim, M. K. A., Miryala, M., Baqiah, H., Shariff, K. K. M., Hong, Y. S., & Mohamed, A. R. A. (2024). Comparative studies of pure $YBa_2Cu_3O_{7-\delta}$ prepared by modified thermal decomposition method against thermal treatment method. *Applied Physics A*, *130*(5), 340. https://doi.org/https://doi.org/10.1007/s00339-024-07412-y

Tan, C., Awang Kechik, M., Che Dzulkifli, N., Sukor, S., Kamarudin, A., Yap, S., Baqiah, H., Karim, M., Chen, S., & Lim, K. (2023). Effect of concentration of potassium added in $Y_1Ba_2Cu_3O_{7-\delta}$ superconductor by using the thermal treatment method. *AIP Conference Proceedings*, *2619*(1). https://doi.org/https://doi.org/10.1063/5.0122523

Yap, S., Kechik, M., Chen, S., Kamarudin, A., Baqiah, H., Lim, K., Karim, M., Halim, S., Doyan, A., & Shariff, K. (2023). Comparative study on superconducting properties and surface morphology analysis for $Y_{0.85}K_{0.15}Ba_2Cu_3O_{7-\delta}$ and $Y_{0.85}Ca_{0.15}Ba_2Cu_3O_{7-\delta}$ synthesized via thermal treatment method. AIP Conference Proceedings,

Yap, S. H., Awang Kechik, M. M., Alhadei Mohamed, A. R., Baqiah, H., Chen, S. K., Lim, K. P., Zailani, T. H., Shabdin, M. K., Mohd Shariff, K. K., Yaakob, Y., Mohd Zaid, M. H., Abdul Karim, M. K., Hisamuddin, N. F., Humaidi, S., Tan, K. B., Shaari, A. H., & Miryala, M. (2025). Comparing study of electrical transport properties of bulk Y-123 synthesized by modified wet and dry synthesis methods. *Solid State Sciences*, *164*, 107921. https://doi.org/https://doi.org/10.1016/j.solidstatesciences.2025.107921

Yap, S. H., Awang Kechik, M. M., Baqiah, H., Chen, S. K., Lim, K. P., Shabdin, M. K., Mohd Zaid, M. H., Yaakob, Y., Abdul Karim, M. K., Loh, Z. W., Shaari, A. H., & Miryala, M. (2024). Comparative study of superconducting properties for $YBa_2Cu_3O_{7-\square}$ added Ca-compounds synthesised under different annealing conditions. *Solid State Science and Technology*, *31*(2), 71-81. https://myjms.mohe.gov.my/index.php/masshp/article/view/25684

Yap, S. H., Awang Kechik, M. M., Mohamed, A. R. A., Khoerunnisa, F., Baqiah, H., Chen, S. K., Lim, K. P., Shabdin, M. K., Humaidi, S., Mohd Zaid, M. H., Yaakob, Y., Abdul Karim, M. K., Tan, K. B., & Shaari, A. H. (2025). Exploring the impact of ambient annealing on the superconducting properties of Y-123 with marine waste-derived chitosan additives. *Ceramics International*. https://doi.org/https://doi.org/10.1016/j.ceramint.2025.06.360

Yap, S. H., Kechik, M. M. A., Khoerunnisa, F., Baqiah, H., Chen, S. K., Lim, K. P., Shabdin, M. K., Zaid, M. H. M., Yaakob, Y., Karim, M. K. A., Humaidi, S., Shaari, A. H., & Miryala, M. (2024). Microstructural and excess conductivity properties of Y-123: effect of organic polymer chitosan inclusion. *Journal of Materials Science: Materials in Electronics*, *35*(21), 1452. https://doi.org/10.1007/s10854-024-13161-8

Yap, S. H., Kechik, M. M. A., Shariff, K. K. M., Baqiah, H., Chen, S. K., Lim, K. P., Shabdin, M. K., Zaid, M. H. M., Yaakob, Y., Karim, M. K. A., Humaidi, S., Shaari, A. H., & Miryala, M. (2024). Fluctuation induces conductivity and microstructural studies in Y-123: Effect of CaO inclusion. *Journal of Alloys and Compounds*, *1005*, 175955. https://doi.org/https://doi.org/10.1016/j.jallcom.2024.175955